

# Lip Leakage Flow Simulation for the Gravity Probe B Gas Spinup

Leonardo Dagum\*

Computer Sciences Corporation, Moffett Field, California 94035

The lip leakage flow for the Gravity Probe B (GP-B) gas spinup system is investigated using a particle simulation code on the Connection Machine. Particle simulation is employed because the flow conditions are in the transition regime between continuum and free-molecular conditions where particle methods are applicable. The dominant flow is Couette in nature and the simulation is first validated through comparison to theoretical results for Couette flow in the transition regime. A GP-B-type geometry is then simulated and results are presented for two conditions, those corresponding to the area near the inlet and near the outlet of the spinup channel. The finite width of the channel lip leads to a lower drag than would be predicted by assuming Couette flow.

## Nomenclature

$\delta$	= distance between plates in Couette flow
$\lambda$	= mean free path
$\tau$	= shear stress
$a$	= speed of sound
$C$	= velocity component
$f$	= distribution function
$K_n$	= Knudsen number
$k$	= Boltzmann's constant
$M$	= Mach number
$m$	= molecular mass
$n$	= number density
$T$	= temperature
$Q$	= flux quantity
$w$	= velocity component in $z$ direction

## Subscripts

$o$	= reference condition, spinup channel (or initial) condition
FM	= free molecule condition
gyro	= gyro condition
$i$	= $i$ th component
$n$	= normal direction
$t$	= tangential direction
$w$	= wall condition

## I. Introduction

**G**RAVITY Probe B (GP-B) is an effort to experimentally validate the general theory of relativity. The basis of the experiment is to measure any coupling of Earth's gravitational tensor with the angular momentum of four spherical gyroscopes placed in a drag-free orbit about the Earth. The experiment has been reviewed in Ref. 1 and will not be discussed here. The aspect of the experiment which is of concern in this work is the spinup system. One of the long-standing challenges of the GP-B effort has been to design a system which can spin the rotors of the gyroscopes to 170 Hz at temperatures below 9K (the transition temperature of the superconducting niobium film coating on the gyroscopes).

The proposed spinup system is described by Xiao.<sup>2</sup> The spinup system is constrained to fit into the current design of the experiment and certain conditions are required:

- 1) The system must operate at temperatures below 9K.
- 2) The gas leakage rate must be less than  $70\mu\text{g/s}$ .
- 3) The gas flow rate must be less than 2 mg/s with an exhaust pressure of 0.35 Torr or higher.
- 4) The system should operate at a background pressure as high as 0.4 millitorr.

The difficulty arises in meeting the second constraint. This constraint is fixed by the size of the vacuum lines which will evacuate the system.

The system consists of a single spinup channel and a sonic nozzle (see Fig. 1). The spinup channel is surrounded by a larger auxiliary channel. The channels are cut from the inner side of the gyroscope housing, and the gyroscope surface acts as the fourth wall. Figure 1 consists of a cross-sectional and a plan view of the gyroscope and gyroscope housing around the spinup and auxiliary channels. The top figure is the cross-sectional view. The hashed line represents the gyroscope. The

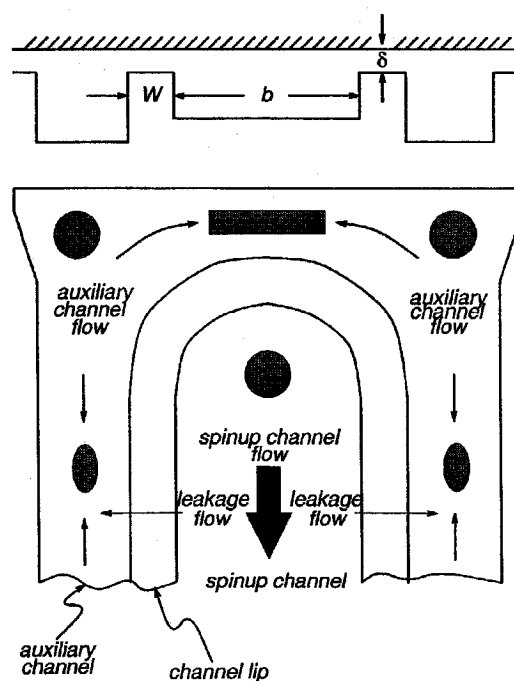


Fig. 1 Spinup channel and gyroscope.

\*Presented as Paper 92-0559 at the AIAA 30th Aerospace Sciences Meeting, Reno, NV, Jan. 6-9, 1992; received March 30, 1992; revision received July 5, 1993; accepted for publication Aug. 25, 1993. Copyright © 1993 by the American Institute of Aeronautics and Astronautics, Inc. All rights reserved.

Research Scientist, Member AIAA.

bottom figure is the plan view. The shaded areas in the auxiliary channel represent sinks in the auxiliary channel flow. These are connections to the pumping system; the arrows indicate the direction of flow. The shaded area in the spinup channel represents a source in the spinup channel flow. This is the outlet of a nozzle which impinges helium on the gyroscope causing it to rotate in the direction of the wide arrow in the figure. The arrows from the spinup channel to the auxiliary channel indicate the direction of the leakage flow; that is, the flow which leaks from the spinup channel through the channel lip.

The flow in the gyroscope spinup system can be divided into four sections: flow in the spinup channel, flow over the channel lip, flow in the auxiliary channel, and flow in the rest of the housing. The flow in the spinup channel is in the continuum regime, and the flow in the auxiliary channel and in the rest of the housing is in the free-molecular regime. Therefore these sections of the analysis can be carried out without great difficulty by applying the well-established equations governing flow in those regimes. However, the flow over the channel lip is in the transition regime between continuum and free-molecular flow. This flow is best handled through a particle simulation. Because of the very close spacing between the housing and the gyroscope, the shear stress on any gas flowing through this gap will be much higher than anywhere else in the gyroscope. It is expected that the lip leakage flow will contribute up to 80% of the parasitic drag in the spinup. It is very important to have a good model of this flow since excessive parasitic drag must be overcome by a greater nozzle flow rate which is constrained by the pumping system.

PSiCM is a highly optimized, three-dimensional particle simulation implemented on the Connection Machine at the Numerical Aerodynamic Simulation facility in the NASA Ames Research Center. The code incorporates the same physics of the direct simulation Monte Carlo (DSMC) method pioneered by Bird<sup>3</sup> but makes use of the collision selection rule described in Ref. 4. Details of the parallel algorithms employed in PSiCM may be found in Refs. 5 and 6.

For this work PSiCM was only used in the two-dimensional mode. A two-step approach was undertaken towards simulating the lip leakage flow. The first step was to properly model the particle/surface interaction at the conditions of interest. For this purpose, PSiCM was set up to simulate a Couette flow at the very low temperatures under consideration. This afforded a useful comparison of the simulation to theory, since Couette flow is well-understood throughout the transition regime and approximate analytical models do exist (for example, see Ref. 7). Once the Couette flow problem was properly handled by the simulation, the channel lip geometry was simulated and drag and leakage rate data collected. Concurrent with this work, an experimental investigation of the gas spinup system is being carried out at Stanford University, and a comparison of simulation results with experimental results will be possible when those become available. The simulation results presented here have succeeded in providing a better understanding of the leakage flow and aided in the design of the experiment.

## II. Particle/Surface Interaction Model

The particle/surface interaction model used for these simulations is the perfectly diffuse reflection model<sup>3</sup> first proposed by Maxwell in 1879. In a perfectly diffuse reflection, a particle striking the surface is assumed to remain trapped on the surface for sufficient time to lose all relation to its preinteraction state. The reflected direction of a particle is completely independent of its incident direction and the probability of a particular reflected direction is proportional to the cosine of the reflection angle (measured from the surface normal). Furthermore, the reflected gas is assumed to have acquired a temperature equal to that of the surface. In the simulation, a reflected particle's tangential velocity components are sampled from a Maxwellian distribution at the surface temperature, and the normal velocity component is sampled from the distribution function for flux

across a plane. This is equivalent to treating the element of surface area as a transparent plane with a Maxwellian gas at rest and at the surface temperature behind it. The reflected particles move from this gas into the flow through the transparent plane.

The Maxwellian distribution  $f$  is given by (see Ref. 7)

$$f(C_i) = \left( \frac{m}{2\pi kT} \right)^{3/2} \exp \left[ -\frac{m}{2kT} (C_1^2 + C_2^2 + C_3^2) \right] \quad (1)$$

This distribution is used to sample velocity components tangential to the surface. Clearly there is no bias on the particles in the tangential direction and the tangential velocity distribution of particles crossing a plane in an equilibrium gas must be given by the Maxwellian distribution. In the normal direction, however, the Maxwellian distribution cannot be used because not all particles in the equilibrium gas are equally likely to cross the plane. The normal velocity distribution of particles crossing a plane can be deduced by considering the number flux across the plane. The flux across a plane of any quantity  $Q$  is given by (cf. Ref. 3)

$$n \langle Q C_n \rangle \quad (2)$$

where the angle brackets are used to denote a mean quantity. For an equilibrium gas with velocity distribution  $f$ , the number flux is given by setting  $Q = 1$  and integrating

$$n \int_{-\infty}^{\infty} \int_{-\infty}^{\infty} \int_0^{\infty} C_n f dC_n dC_t \quad (3)$$

It follows that the normal velocity distribution  $f_n$  for particles crossing a plane must be given by the integrand of Eq. (3), or

$$f_n(C_n) = C_n f(C_n) \quad (4)$$

## III. Model Validation—Couette Flow Results

As mentioned earlier, a Couette flow simulation was carried out to validate the models used. Couette flow appeared as a very appropriate model problem for several reasons. Most importantly, approximate analytical solutions exist (see Ref. 7) and these can be used for comparison with the simulation results. In addition, Couette flow is essentially a degenerate case of the lip leakage flow obtained when equal pressure exists in the spinup channel and the auxiliary channel. Therefore, by correctly simulating Couette flow at the conditions of interest for the GP-B experiment, one can feel confident in the simulation results for the lip leakage flow. In this way the Couette flow problem is used to validate the particle/surface interaction model, the geometry of the simulation, and the chosen particle interaction potential.

Although Couette flow is one-dimensional in nature, the Couette flow simulation was carried out in a two-dimensional geometry of approximately the same dimensions as was later used for the lip leakage simulation. This was useful in determining appropriate parameters for running the lip leakage simulation. The Couette geometry used a rectangular cell network of dimensions  $250 \times 32$  and was initialized with 16 particles per cell (see Fig. 2). The upper boundary was stationary and

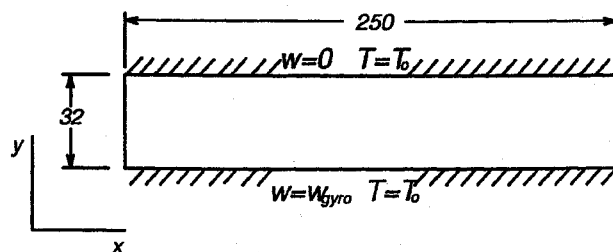


Fig. 2 Geometry for Couette flow simulation.

assumed to be isothermal at the initial gas temperature (which corresponded to 7° K). The lower boundary was also isothermal and at the gas temperature but moving in the  $z$  direction (out of the plane of Fig. 2) at a fixed velocity  $w_{gyro}$ . To speed up the transient, the particles were initialized with a linear gradient from 0 to  $w_{gyro}$  in the  $z$  velocity component. This was especially useful at very small Knudsen numbers where, with a subsonic Mach number, the velocity diffusion from the moving surface can be exceedingly slow.

On a typical run, 2900 time steps were carried out to reach steady-state conditions. The particles were then cloned twice and 100 time steps were carried out to eliminate any statistical dependencies from the cloning. Following this, the simulation was run for 1500 time steps with sampling on every time step (corresponding to about  $10^5$  samples per cell) to generate a solution. Figure 3 presents the drag on the moving wall (normalized by the drag in the free-molecular limit) as a function of the Knudsen number. The Knudsen number for these flows was defined as

$$K_n = \lambda_0 / \delta \quad (5)$$

Results were obtained for Maxwell, hard-sphere, and inverse 9th power law interaction potentials. Power law potentials were simulated using the variable hard-sphere model.<sup>8</sup> The wall Mach number was 0.333 and the Knudsen number ranged from 0.031 to 10.0. The simulation results are shown compared to Lees' theoretical results as given in Ref. 7. Lees' solution assumes a hard-sphere potential and the good agreement between the hard-sphere simulation and Lees' solution indicates that the simulation is accurate.

Viscosity of helium at low temperatures has been carefully measured in Ref. 9. Since the temperature variation in the GP-B flowfield is small, the choice of potential does not greatly affect the results so long as the reference viscosity is accurate. For reasons of simplicity, then, a hard-sphere potential was chosen for the GP-B simulations with the reference viscosity set correctly<sup>9</sup> for helium at 7 K.

Figure 4 shows the velocity profiles (normalized by  $w_{gyro}$ ) for the hard-sphere interaction potential with a moving wall Mach number of 0.333 and Knudsen numbers ranging from 0.031 to 10.0. The results were generated by ensemble averaging across the 250 columns of cells in the two-dimensional geometry. The profiles are all relatively flat, as would be expected for such low Mach numbers. Furthermore, the intersection point for all the profiles is at  $w/w_{gyro} = 0.5$  and  $y/\delta = 0.5$ , again as would be expected.

Figure 5 shows the shear stress profiles normalized by the free-molecular value. These results again are for the hard-sphere

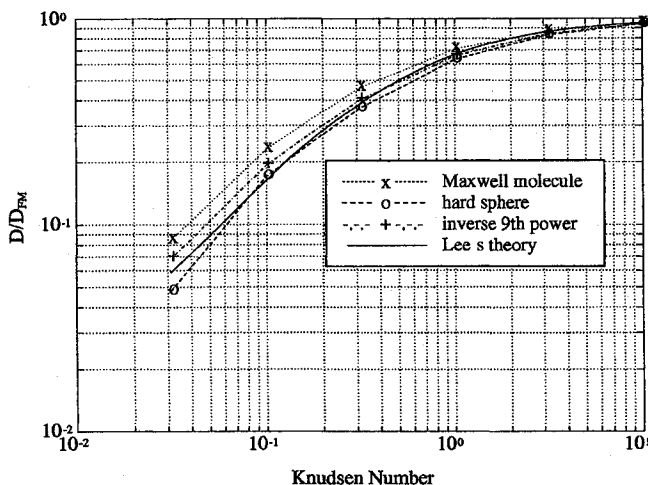


Fig. 3 Normalized drag on moving surface in Couette flow as function of Knudsen number; drag is normalized by the value in the free-molecular limit.

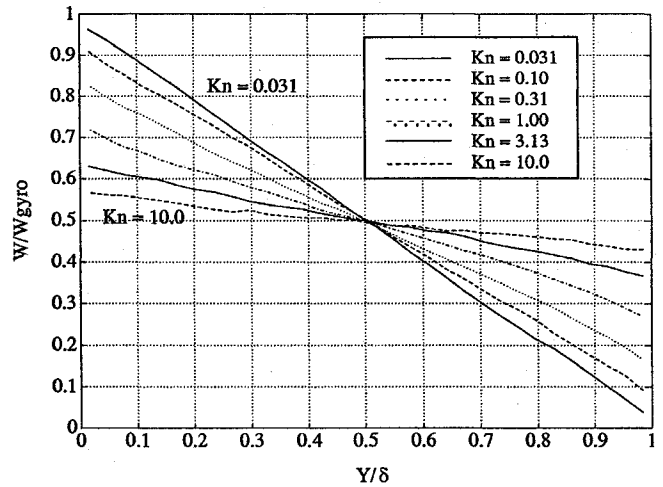


Fig. 4 Velocity profiles as a function of Knudsen number for Couette flow with hard-sphere interaction potential.

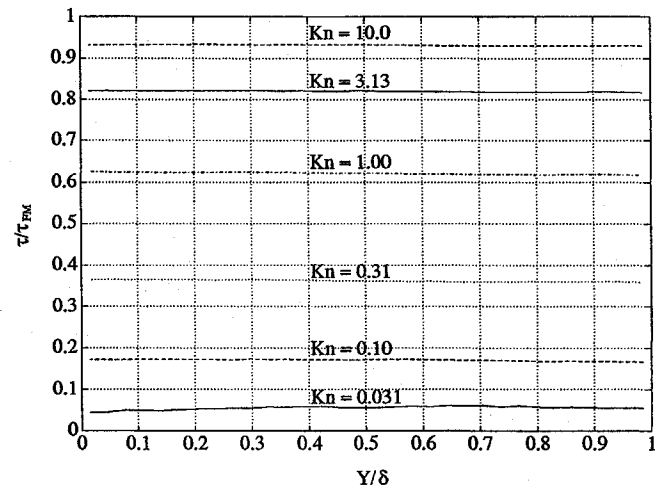


Fig. 5 Couette shear stress profiles as a function of Knudsen number for a hard-sphere interaction potential; shear stress is normalized by the free-molecular value, position is normalized by the width between the moving and the stationary plate  $\delta$ .

interaction potential and moving wall Mach number of 0.333. It is encouraging to see such flat profiles, especially near the boundaries. Because the shear stress is a second moment of the velocity distribution, it is particularly susceptible to small disturbances in the gas. The absence of disturbances near the boundaries indicates that they are being handled correctly by the simulation. The shear stress profile at the lowest Knudsen number considered ( $K_n = 0.031$ ) is not as flat as would be desired. At these conditions (i.e., near-continuum and subsonic) it becomes very difficult to generate good solutions because the velocity distributions defined by the particles are subject to large statistical error. At this point one is better served by considering continuum methods of solution.

#### IV. Gravity Probe B Simulation—Geometry and Relevant Parameters

The GP-B geometry was approximated as shown in Fig. 6. The spinup channel is modeled by the rectangular  $80 \times 32$  chamber in the left of the figure. The channel lip is modeled by the  $350 \times 16$  chamber to the right of this, and the auxiliary channel is modeled by the  $80 \times 32$  chamber at the right end of the figure. The aspect ratio of the channel lip is 21.9; this value was chosen to correspond with the experimental setup which is to use a gap width of 0.023 mm and a gap length of 0.50 mm. The hashed boundaries are diffusely reflecting and

at a fixed temperature  $T_0$ . The lower boundary is allowed to move in the  $z$  direction (out of the plane of Fig. 6) at velocity  $w_{gyro}$  while the upper boundary is fixed. The boundary at the right-hand end of the figure is an exit boundary. All particles crossing that boundary are removed from the flow. The remaining six boundaries are specularly reflecting.

The flow of interest for these simulations is the lip leakage flow (see Fig. 1). Particles were initialized with temperature  $T_0$ , pressure  $p_0$ , and initial flow velocity  $w_0$  in the  $z$  direction. The flow was initialized only in the spinup and lip chambers, each with an initial number density  $n_0$  of 13 particles per cell. The auxiliary chamber was evacuated. The simulation was run for 3900 time steps to clear the transient; then particles were cloned three times, thus increasing the total number of particles by a factor of eight. The simulation was run for another 100 time steps before time averaging began. Time averaging was carried out for 1500 time steps with samples collected at every time step. Typically, there were some  $7.5 \times 10^5$  particles in the flow for the time averaging phase.

During the calculation, new particles were introduced in the spinup chamber at the initial conditions and at a mean fill rate of  $n_0/10$  particles per time step. The fill rate was an input value for these simulations. Since the conditions for the simulations all lead to choked flow, the results were fairly insensitive to the fill rate.

Two sets of runs were carried out; the relevant parameters are listed in Tables 1 and 2. The first set of runs corresponded to conditions near the inlet of the spinup channel and the second set of runs corresponded to conditions near the outlet of the spinup channel (see Fig. 1). The values are listed in simulation units. In both sets of runs, the gas temperature and pressure were held fixed while the gyroscope's velocity was varied. Drag on the gyroscope was measured only in the channel lip and auxiliary channel.

Table 1 Relevant parameters for simulations corresponding to conditions near the inlet of the spinup channel

Run	$a_0$ , cells/step	$w_0$ , cells/step	$M_{z_0}$	$\lambda_0$ , cells	$T_w/T_0$	$w_{gyro}$ , cells/step
1	0.15	0.05	0.33	1.0	1.0	0.00
2	0.15	0.05	0.33	1.0	1.0	0.005
3	0.15	0.05	0.33	1.0	1.0	0.01
4	0.15	0.05	0.33	1.0	1.0	0.02
5	0.15	0.05	0.33	1.0	1.0	0.03
6	0.15	0.05	0.33	1.0	1.0	0.04
7	0.15	0.05	0.33	1.0	1.0	0.05

Table 2 Relevant parameters for simulations corresponding to conditions near the outlet of the spinup channel

Run	$a_0$ , cells/step	$w_0$ , cells/step	$M_{z_0}$	$\lambda_0$ , cells	$T_w/T_0$	$w_{gyro}$ , cells/step
1	0.15	0.075	0.5	1.6	1.0	0.00
2	0.15	0.075	0.5	1.6	1.0	0.01
3	0.15	0.075	0.5	1.6	1.0	0.02
4	0.15	0.075	0.5	1.6	1.0	0.03
5	0.15	0.075	0.5	1.6	1.0	0.04
6	0.15	0.075	0.5	1.6	1.0	0.05

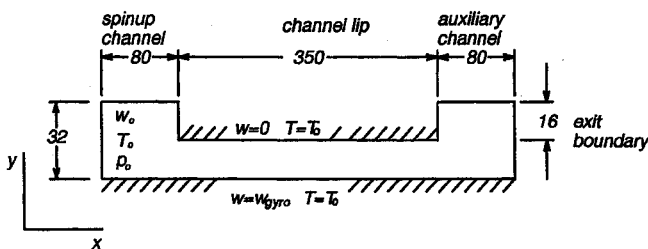


Fig. 6 Geometry for Gravity Probe B simulation.

Table 3 lists the assumed conditions for the inlet and outlet of the spinup channel. These values may be used to convert from simulation units to physical units. Note that for the near-inlet conditions, the geometry of Fig. 6 leads to a channel lip length ( $x$  direction) of 0.38 mm rather than the 0.50 mm expected for the experiment. The simulation does not provide reliable results with mean free paths smaller than 1.0 cells; consequently, it was not possible to exactly simulate the near inlet conditions. To first order, one can correct for this in the drag measurements by scaling the drag results with a factor of 0.50/0.38.

## V. Gravity Probe B Simulation—Results

Figure 7 presents the results for the drag on the gyroscope in the channel lip and auxiliary channel sections as a function of the gyroscope velocity normalized by  $w_0$  at the near-inlet conditions. The drag is normalized by unit depth (i.e., in the  $z$  direction). As expected, the drag increases linearly with the gyroscope velocity. The observed deviations from linearity are attributable to the statistical nature of solutions generated by a particle simulation. This is especially noticeable in the near-inlet calculations where the Mach number in the spinup channel was only 0.33, making it difficult to obtain a clean solution. Furthermore, as described in the previous section, the equivalent length ( $x$  direction) of the channel lip was shorter for the near-inlet simulations and this was accounted for as described in that section.

A least squares fit was made of the data points and the resulting lines are shown in the figure. Note that the lines do not pass through the origin. For a Couette flow one would expect the drag to go to zero for a zero plate velocity. This is not the case for the GP-B geometry because the plates are not infinite (in the  $x$  direction). With plates of finite length one has to consider the effects of the velocity profiles at either end of the plates. In the present case, gas is introduced at the spinup side with some bulk velocity in the  $z$  direction, and the gas that leaks through the channel lip has some momentum in the  $z$  direction. Consequently, when the gyroscope is stationary there is momentum imparted to it by the leakage gas in the

Table 3 Experimental conditions near the outlet and the outlet of the spinup channel

Position	$T_0$ , K	$T_w$ , K	$M_z$	$P_0$	$\lambda_0$ , $\mu\text{m}$
Near inlet	7.0	7.0	0.33	227	1.1
Near outlet	7.0	7.0	0.50	107	2.0

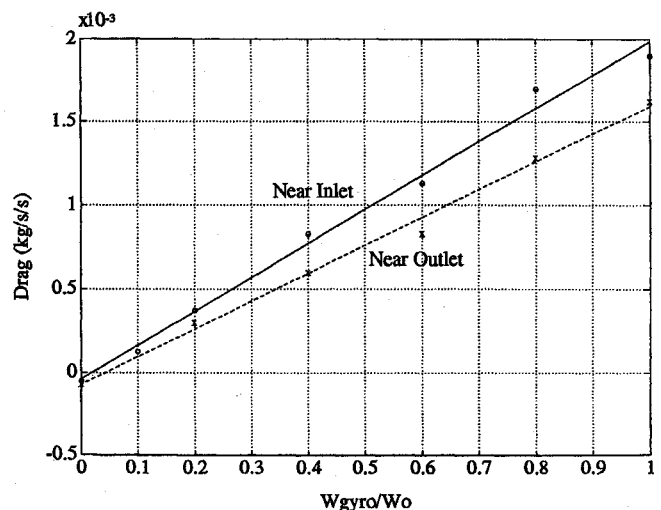


Fig. 7 Lip leakage flow drag in Gravity Probe B simulation as a function of the normalized gyroscope velocity.

channel lip section. This effect should become more pronounced for a shorter-length channel lip.

Figure 8 presents the shear stress through the channel lip for the near-inlet conditions. Each point in the curves represents the average of 160 cells taken as follows: the 16 rows of cells in the channel lip were averaged, then each 10 consecutive values in this result were averaged. The shear stress has been nondimensionalized by the free-molecular shear stress for pure Couette flow at the given gyroscope velocity. Note that both in this figure and in Fig. 9 the results for a stationary gyroscope (i.e., run 1 in Tables 1 and 2) are not included because the corresponding free-molecular shear stress in Couette flow is zero. Physical units are used for the channel lip. The channel lip begins at  $x = 0.87 \times 10^{-4}$  m and ends at  $x = 4.71 \times 10^{-4}$  m.

Nondimensionalizing by the free-molecular shear stress tends to collapse the results onto a single curve with an average value through the lip section of 0.044. Pure Couette flow at the same Knudsen number would give a value of 0.11 (see Fig. 3). The simulation result is lower than the pure Couette value because of the finite lip length.

It is of interest to note that because the shear stress is relatively constant throughout the channel lip, the drag from the channel lip will grow in direct proportion to the length ( $x$  direction) of the lip. This supports the use of the correction factor, 0.50/0.38, in computing the drag from the near-inlet simulations.

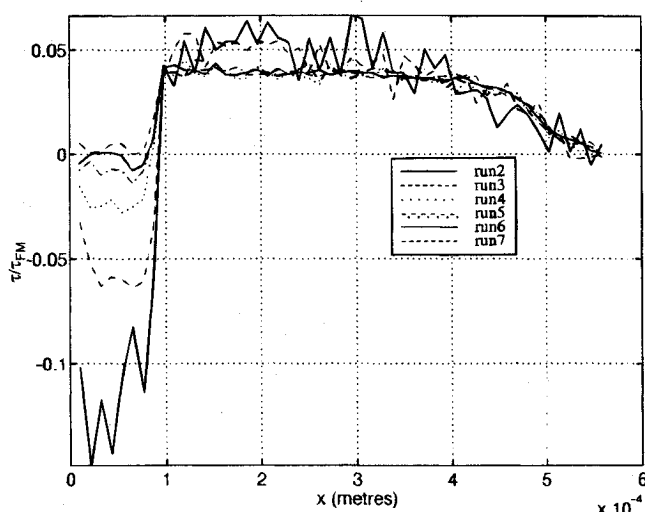


Fig. 8 Shear stress through the channel lip section for near-inlet conditions; run numbers identified in Table 1.

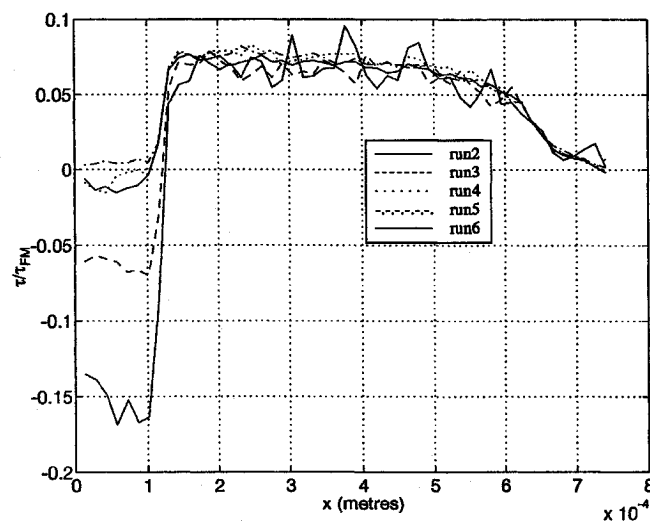


Fig. 9 Shear stress through the channel lip section for near-outlet conditions; run numbers identified in Table 2.

Figure 9 presents the shear stress through the channel lip for the near-outlet conditions. This figure was created using the same averaging as in Fig. 8. The channel lip begins at  $x = 1.16 \times 10^{-4}$  m and ends at  $x = 6.25 \times 10^{-4}$  m. The near-outlet conditions were simulated by increasing the bulk velocity  $w_0$  in the spinup channel. The range for the gyroscope velocity was the same as with the near-inlet conditions. Note that in form, the shear stress curves of Fig. 9 are similar to those of Fig. 8, however the higher gas velocity in the spinup channel reduces the shear stress in the channel lip and results in a correspondingly reduced drag (see Fig. 7). The nondimensional shear stress is greater, however, because of the greater Knudsen number ( $K_n = 0.10$ ) for the near-outlet conditions. The average value for the nondimensional shear stress in the lip section is 0.071; for pure Couette flow one computes a nondimensional shear stress of 0.17 (see Fig. 3).

Of interest for the GP-B experiment is the leakage rate of the spinup system. As was mentioned earlier, the conditions for the simulation resulted in a choked flow so the leakage rate (that is, the rate at which particles exit the simulation) was constant for both the near-inlet and near-outlet conditions. For near-inlet conditions the mean leakage rate was 23.7 particles per cell per unit depth. In physical units this corresponds to 4.05 mg/s per meter depth. Since the actual spinup channel measures 2.327 cm, this implies a leakage rate of 0.096 mg/s per side or 0.192 mg/s in total. For the near-outlet conditions, the simulation mean leakage rate was 23.0 particles per cell per unit depth which, through a similar calculation, converts to a total leakage rate of 0.116 mg/s. The difference between the two results is due, in part, to the different lengths of gap in the two cases. Recall that the near-inlet conditions simulated a gap of length 0.38 mm whereas the near-outlet conditions simulated a gap of length 0.50 mm. The shorter gap allows a greater leakage rate but also produces less drag. Clearly there is a design tradeoff in the gap length which should be addressed.

The calculations presented here were carried out on the Connection Machine Model CM-2 at the NASA Ames Research Center. The machine consists of 32,768 bit serial processors and 1024 64-bit Weitek floating point units. Each bit serial processor has 128 kB of memory and the machine in total has 4 GB of memory. The calculations were run using only half of the available processors and each calculation on the GP-B geometry required about 90 minutes to complete. For comparison with other calculations the normalized units of time per particle per time step is often used. This value was  $3.3 \mu\text{s}/\text{particle}/\text{step}$  during the transient phase and  $2.8 \mu\text{s}/\text{particle}/\text{step}$  during the time averaging phase. The lower performance during the transient phase is due to the lower virtual processor ratio used in that part of the calculation (this is discussed in Ref. 5). Using the whole machine (i.e., all 32,768 processors) would approximately halve these times. By comparison, one processor of the Cray Y-MP running the fully vectorized equivalent of PSICM typically obtains  $1.0 \mu\text{s}/\text{particle}/\text{step}$  and is about 40% faster than the CM-2 for these calculations.

## VI. Conclusions

This paper presents preliminary results in the investigation of the lip leakage flow of a proposed gas spinup system for the GP-B experiment using a particle simulation for rarefied flows. The investigation has been carried out in two steps. The first step has been the validation of the method by comparison of simulation results with known theoretical results for Couette flow, which is expected to be dominant in the experiment. The second step has been to carry out simulations of the leakage flow for a GP-B-type geometry at the conditions expected for the experiment. These simulation results have yielded greater insight into the flow and have been of use to researchers designing a land-based experiment to study the spinup system. When these experimental data become available it will be possible to further validate the method and then use the simulation to investigate the effect of the spinup channel geometry on the

leakage flow (an issue which is left completely untouched in the present work) and to assess the tradeoff between gap length and leakage rate.

### Acknowledgments

This work is supported through NASA Contract NAS 2-12961. The author would like to gratefully acknowledge Yeuming Xiao for many helpful discussions with regard to the proposed spinup system.

### References

- <sup>1</sup>Everitt, C. W. F., "The Stanford Relativity Gyroscope (A): History and Overview," *Near Zero: New Frontiers of Physics*, edited by J. D. Fairbank, B. S. Deaver, C. W. Everitt, and P. F. Michelson, W. H. Freeman and Co., New York, 1988, pp. 587-639.
- <sup>2</sup>Xiao, Yeuming, "A Low Pressure Gas Spinup System for GP-B Gyroscope," GP-B TR S0136, Dept. of Applied Physics, Stanford Univ., Stanford, CA, May 1990.

<sup>3</sup>Bird, G. A., *Molecular Gas Dynamics*, Clarendon Press, Oxford, England, UK, 1976.

<sup>4</sup>Baganoff, D., and McDonald, J. D., "A Collision-Selection Rule for a Particle Simulation Method Suited to Vector Computers," *Physics of Fluids A*, Vol. 2, No. 7, 1990, pp. 1248-1259.

<sup>5</sup>Dagum, L., *On the Suitability of the Connection Machine for Direct Particle Simulation*, Ph.D. Thesis, Dept. of Aeronautics and Astronautics, Stanford Univ., Stanford, CA, 1990.

<sup>6</sup>Dagum, L., "Three Dimensional Direct Particle Simulation on the Connection Machine," *Journal of Thermophysics and Heat Transfer*, Vol. 6, No. 4, 1992, pp. 637-642.

<sup>7</sup>Vincenti, W. G., and Kruger, C. H., *Introduction to Physical Gas Dynamics*, Robert E. Krieger Publishing Co., 1965.

<sup>8</sup>Bird, G. A., "Monte-Carlo Simulation in an Engineering Context," *Proceedings of 12th International Symposium on Rarefied Gas Dynamics* (Charlottesville, VA), 1980, pp. 239-255.

<sup>9</sup>McCarty, R. D., "Thermophysical Properties of Helium-4 from 2 to 1500K with Pressures to 1000 Atmospheres," National Bureau of Standards TN-631, 1972.

Gerald T. Chrusciel  
Associate Editor